1st International Symposium on Naval Architecture and Maritime
YTU campus, Istanbul (INT-NAM 2011) on October 24-25, 2011.

Guidelines for Numerical Flow Simulation around Marine Propeller

Prof. Mosaad M. A., Port Said University, Egypt, mamosaad2000@yahoo.com

Prof. Mosleh M., Alexandria University Egypt momosleh@gmail.com

Ass. Prof. Dr. El-Kilani H. Port Said University, Egypt hebaelkilani@gmail.com

Dr. Yehia,W. Port Said University, Egypt waleed.yehia@gmail.com

Abstract

The flow around a marine propeller is one of the most challenging hydrodynamics problems. Computational fluid dynamics (CFD) has emerged as a potential tool in recent years and has promising applications. The goal of this paper is to provide complete guidelines for geometry creation, boundary conditions setup, and solution parameters of the flow around rotating propeller. These guidelines are addressed to handle propeller simulation problems in order to achieve quick, more accurate solution with less computational cost. In this paper CFD results for flow around a marine propeller are presented. Computations were performed for various advance ratios following experimental conditions. Reynolds-Averaged Navier-Stokes (RANS) method combined with an extensive validation of two different turbulence models k–ε and k–ω was applied for the flow simulation. The computations enable direct comparison of the reliable CFD results with the experimental data.

Key-Words: - Propeller flow, CFD simulation, RANS

1. Introduction

The flow around the propeller is complex due to its geometry and the combined rotation and advancement into water. The availability of numerical techniques and low cost high-speed computational capability has made a major impact on the analysis of complex flows. Computational fluid dynamics with regard to these specific applications is still in a process of evolution, as is evidenced from specific validation studies in current research literature.

RANS computations offer that possibility, and such viscous-flow computations start to be used in the practical ship design; but how accurate these predictions are, and to what extent they depend on the turbulence modelling used, is not really known [1]. Despite of the great advancement in the CFD technologies and feasibilities of the approaches for marine propeller flows, some issues need to be addressed for more practicable procedures. The complexity in geometry, mesh generation and turbulence modelling are the main obstacles. In fact a marine propeller is a very complex geometry, with variable section profiles, chord lengths and pitch angles, and in operational conditions it induces rotating flow and entails tip vortex [2].

In order to verify the reliability of the CFD simulations, the flow about a propeller model DTMB-P4119 propeller is investigated, and the results are compared with the existing available experimental results.

2. Basic Methodology

Numerical studies were carried out using computational fluid dynamics [FLUENT R12] to obtain the open water characteristics of propeller model as well as the distribution of pressure on the blade surface. This effort involves standardization of the computational grid domain with proper choice of the grid size and control volume around the propeller under investigation.

The general conservative form of the Navier – Stokes equation is presented as the continuity equation

Continuity equation,

$$\frac{\partial \rho}{\partial t} + \frac{\partial}{\partial x_i}(\rho u_i) = S_m \qquad (2.1)$$

Where:

ρ = density, kg/m^3

u_i = is the velocity component in the ith direction, m/s

(i =1, 2, 3) and

S_m = source terms.

In case of incompressible flows the density is considered to be constant. Since the propeller flow has been considered as steady and incompressible, the continuity equation gets modified as,

$$\frac{\partial}{\partial x_i}(\rho u_i) = 0 \qquad (2.2)$$

The momentum equation will be,

$$\frac{\partial}{\partial t}(\rho u_i) + \frac{\partial}{\partial x_j}(\rho u_i u_j) = -\frac{\partial p}{\partial x_i} + \frac{\partial \tau_{ij}}{\partial x_j} + \rho g_i + F_i \qquad (2.3)$$

Where:

$$\tau_{ij} = [\mu(\frac{\partial u_i}{\partial x_j} + \frac{\partial u_j}{\partial x_i})] - \frac{2}{3}\mu \frac{\partial u_l}{\partial x_l}\delta_{ij}, \quad (2.4)$$

τ_{ij} = is the Reynolds stress tensor

p = static pressure, N/m^2

g_i = gravitational acceleration in the ith direction , m/s^2

F_i = external body forces in the ith direction and, N

δ_{ij} is the Kronecker delta and is equal to unity when i=j; and zero when i ≠ j.

The Reynolds-Averaged form of the above momentum equation including the turbulent shear stresses is given by:

$$\frac{\partial}{\partial t}(\rho u_i) + \frac{\partial}{\partial x_j}(\rho u_i u_j) = \frac{\partial}{\partial x_j}\left[\mu\left(\frac{\partial u_i}{\partial x_j} + \frac{\partial u_j}{\partial x_i}\right) - \left(\frac{2}{3}\mu \frac{\partial u_i}{\partial x_i}\right)\right] - \frac{\partial p}{\partial x_i} + \frac{\partial}{\partial x_j}\left(-\rho \overline{u_i' u_j'}\right) \qquad (2.5)$$

Where:

u_i' = is the instantaneous velocity component, m/s (i = 1,2, 3).

In order to characterize turbulence, additional conservation equations (or closure equations) for k–ε and k–ω have to be solved.

3. Geometrical Modeling

The propeller model considered in the present study is DTMB-P4119 designed at the David Taylor Model Basin. P4119 is a three-bladed fixed-pitch propeller of typical diameter D=0.305 m, the geometry data for this propeller was given in [3, 5].

A commercial computer program HydroComp. PropCad used for generation of blade profiles, was used to generate the blade profiles for the geometry of P4119-screw propeller. The program transforms input data into the coordinates of cloud points in space. The points describe the shape of a propeller blade surface and then they can be connected into curves, surfaces and a volume. Propeller data are imported in NURBS (Non-Uniform Rational B Spline) Modeller Rhinoceros 4.0 as a third party program to build a complete solid propeller model. The blades have been simply mounted on an infinitely long cylinder, which serves as the hub and shaft, to avoid the stagnation point on the hub close to the propeller [2, 3]. Figures 3.1, 3.2 show the surface model and solid model respectively.

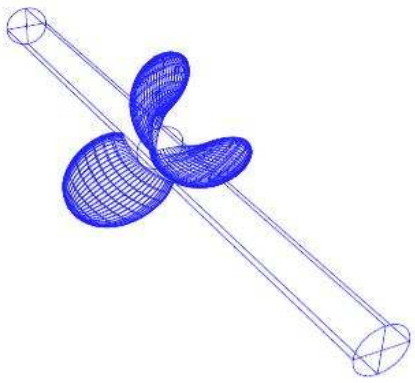

Fig. 3.1 DTMB-P4119 Poly-Surface Model

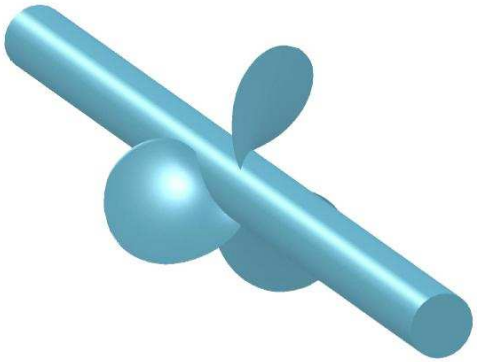

Fig. 3.2 DTMB-P4119 Solid Model

4. Computational Domain

A cylindrical volume is used to simulate the physical domain. The inlet is at 1.5D upstream, the outlet at 3.5D downstream; solid surfaces on the propeller blades and hub are centred at the coordinate system origin and aligned with uniform inflow. The outer boundary is at 1.5 D from the hub. The domain was chosen depending on research performed by [6] and domain dependence studies in [7]. Illustration of the schematic diagram of the propeller computational domain is shown in Fig. 4.1.

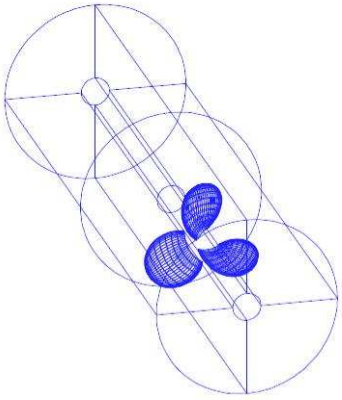

Fig. 4.1 Illustration of Computational Domain

5. Computational Mesh

Unstructured tetrahedral cells were generated using the FLUENT, to define the control volume [7]. Figure 5.1 shows surface meshes on the propeller blade and boss surfaces. The meshes were used to generate a 3-D mesh inside the domain volume; Fig. 5.2 shows the grid in the propeller neighbourhood.

Another important parameter is the quality of the mesh: the elements cannot be too much distorted; otherwise the obtained results will not be correct. It is best to assume the maximum cell equi-angle skew below 0.9 [6].

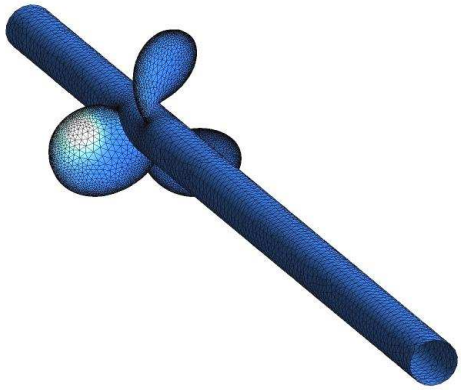

Fig. 5.1 Surface Mesh on Blades and Hub

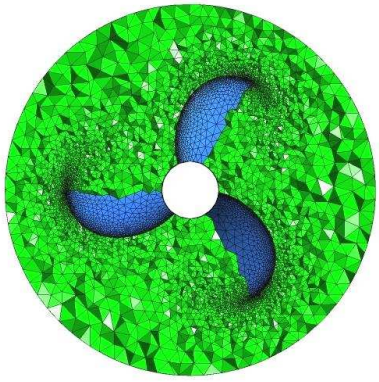

Fig. 5.2 Grid in propeller neighbourhood

6. Boundary Conditions

Boundary conditions were set to simulate the flow around a rotating propeller in open water: A moving reference frame is assigned to fluid with a rotational speed equal to the propeller rpm. Wall forming the propeller blade and hub were assigned a relative rotational speed of zero with respect to adjacent cell zone. A uniform speed according to different advance coefficient was prescribed at inlet. At outlet pressure outlet boundary condition was set. The outer boundary Non-viscous wall was assigned for the outer domain boundary

with relative rotational speed of zero with respect to adjacent cell zone [8].

7. Solver Parameters Setting

The computation conditions were based on the research done by Jessup [4] since the experimental results had been taken from it. The rotational speed was set at 600 rpm. The advance coefficient was changed by changing the velocity of inflow. The computations were performed using two different turbulence models k–ε and k–ω The rotational motion of the propeller was modelled by immobilizing the latter and rotating the calculation domain in the opposite direction this gives exactly the same results as if the propeller were rotating [6]. Computations for one operation point took about 24–48 hr. During this time the program computed about 2000–3000 iterations. Solver parameter settings for the propeller open water simulations including physical constants are shown in Table 7.1.

Table 7.1: Solver Parameters

Parameter	Setting
Solver	3D Segregated, Steady, Implicit
Velocity formulation	Relative to adjacent cell zone
Viscous model	Standard k-ε, k-ω Turbulent model
Water density	998.2kg/m3
Gradient discretization	Green-Gauss Cell Based
Pressure discretization	Body Force Weighted
Momentum discretization	First Order Upwind
Turbulent kinetic energy discretization	First Order Upwind
Turbulence dissipation rate	First Order Upwind
Pressure-velocity coupling	SIMPLE
Blade surface boundary condition	Wall (no slip)
Outer surface boundary condition	Wall (allows slip)
Water inlet boundary condition	Velocity Inlet : Inflow at advance speed
Outflow boundary condition	Pressure outlet

8. Comparison of Results

The open water calculation was carried out at the same running conditions as used in the experimental set up at [4] the calculation was carried out for advance coefficients in the range from 0.5 to 1.1, similar to the experiment. The pressure field on the blades shows low pressure on the suction side; the back of the propeller and high pressure on the pressure side; the face of the propeller. Figures 8.1, 8.2 show the pressure distribution on the both suction and pressure sides respectively for the tested propeller at advance coefficient of 0.5.

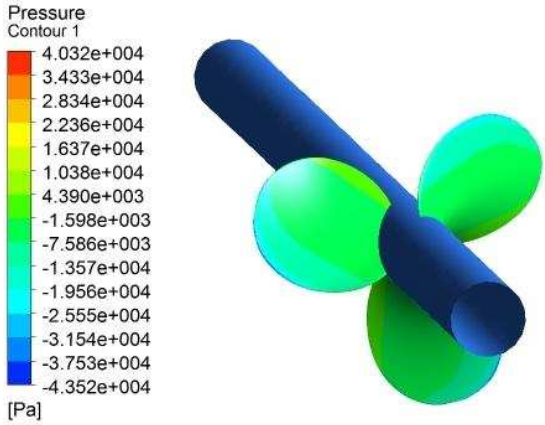

Fig. 8.1 Pressure Distribution on suction side

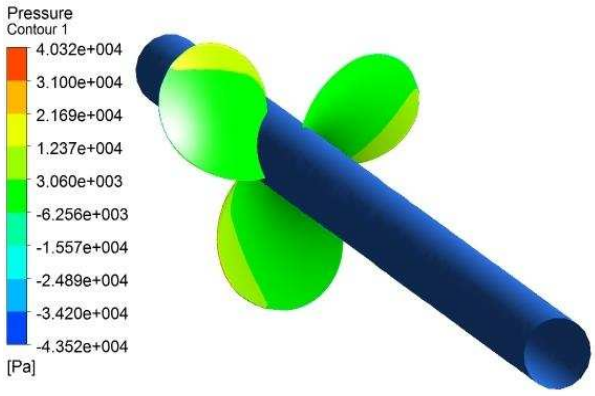

Fig. 8.2 Pressure Distribution on pressure

The study of the flow field shows that the propeller accelerates the flow over the blades and introduces swirl in the flow downstream of the propeller, as expected.

Figures 8.3: 8.7 show the pathlines around the propeller blades. These figures give configurations about how the whirls or wake formed behind the propeller at different advance coefficients.

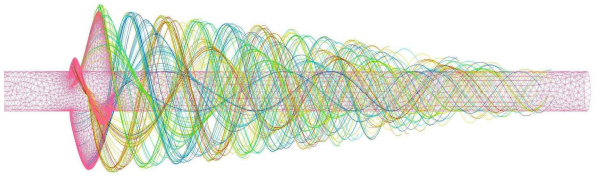

Fig. 8.3 Pathlines around propeller blades at J= 0.5

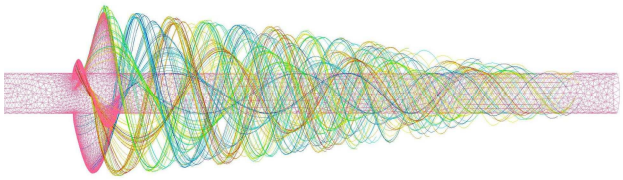

Fig. 8.4 Pathlines around propeller blades at J= 0.7

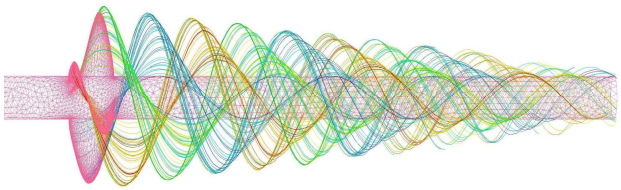

Fig. 8.5 Pathlines around propeller blades J= 0.833

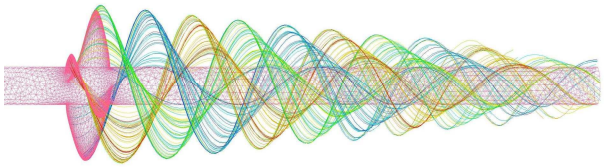

Fig. 8.6 Pathlines around propeller blades at J= 0.9

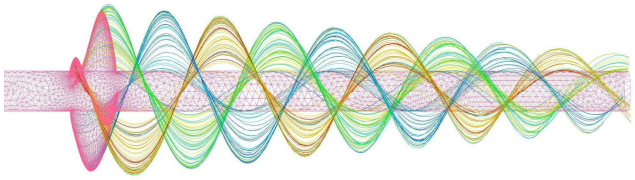

Fig. 8.7 Pathlines around propeller blades at J= 1.1

The thrust and torque coefficients are adequately estimated in comparison with measured data for the range of studied advance coefficients. The computed thrust and torque on the propeller were converted into the dimensionless thrust coefficient, torque coefficient and the efficiency was calculated. Moreover, the study was performed via two turbulence models k-ε, k-ω, and the outcomes of both models were compared with the experimental results conducted by [4] The computation results are presented in Fig. 7.8, which presents the computed thrust, torque coefficients and efficiency, with the corresponding experimental data.

The curves trends with varying advance ratios are well predicted. However, CFD solutions over-predict, and the discrepancy increases with increasing propeller load, i.e., decreasing the advance coefficient, J. This tendency seems to be prevalent in all the RANS CFD simulations and might be unavoidable due to the experimental conditions hardly conformable in CFD, such as the effects of tunnel wall, inflow speed non-uniformity, and hub and boss configurations. [9]

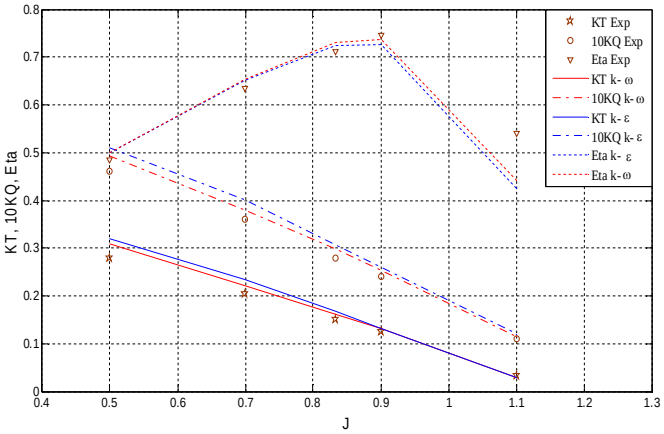

Fig. 7.8 Open water characteristics of DTMB-P4119 propeller

9. Conclusions

The analysis of marine propeller is highly complex which has many consequences, and analyzer must be aware that it is difficult and time-consuming, unless one has a ready methodology of carrying out such investigations. By applying the provided guidelines in this paper quick and correct results can be obtained. Particular focus should be placed in the mesh generation, boundary conditions setup, and turbulence modelling, which reveal to be crucial for the quantitative comparison of the computed results and for the efficiency of the numerical calculations.

CFD results were compared with open water characteristics and found in good agreement. ; Differences between computed and experimental results are less than 5% and 7% for Thrust Coefficient (K_T) and Torque Coefficient (K_Q) while the study considers k-ω as a turbulence model. On the other side, k-ε turbulence model these differences became 7%, 10% for the same parameters respectively. The k-ε model is not quite appropriate for simulating propeller flow because the results in the model have been seen to be over-predicted. The use of a k- ω model is deemed sufficient for propeller applications.

10. References:

[1] Tomasz B., Paweł H., "Numerical Simulation of the Flow around Ship and Rotating Propeller," 18th International Conference on Hydrodynamics in Ship Design, Safety, and Operation, HYDRONAV, Gdańsk, 2010

[2] SILEO, L., BONFIGLIOLI, A., MAGI, V., "RANSEs Simulation of the Flow past a Marine Propeller under Design and Off-design Conditions," 14th Annual Conference Computational Fluid Dynamics Society of Canada (CFD 2006), Queen's University at Kingston, Ontario, Canada, July 16-18, 2006.

[3] SILEO, L., "Low Reynolds Number Turbulent Flow Past Thrusters Of Unmanned Underwater Vehicles," 2nd International Conference on Marine Research and Transportation, ICMRT, Ischia, Naples, Italy

[4] Jessup S. D., "An Experimental Investigation of Viscous Aspects of Propeller Blade Flow," the Catholic University of America, 1989.

[5] Villa D, Gaggero S, Brizzolara S., "A systematic Comparison between RANS and Panel Methods for Propeller Analysis. International Conference on Hydrodynamics, Nantes, France, 2008.

[6] Kulczyk, J., Skraburski, Ł., Zawiślak, M., "Analysis of screw propeller 4119 using the Fluent system," Archives of Civil And Mechanical Engineering ASME, Vol. VII, No 4, 2007

[7] Amminikutty V., Anantha V., Dhinesh G., "Dynamic Characteristics of Marine Hubless Screw Propellers," 5th International Conference, on High Performance Marine Vehicles, 8-10 November, 2006, Australia

[8] Dunna Sridhar, Bhanuprakash T., Das H., "Frictional Resistance Calculations on a Ship using CFD," International Journal of Computer Applications Volume II– No. 5, 2010

[9] RHEE S.H., JOSHI, S., "CFD Validation for a Marine Propeller Using an Unstructured Mesh Based RANS Method," Proceedings of FEDSM'03, the 4th ASMEJSME Joint Fluids Engineering, ASME, Summer Conference, Honolulu, Hawaii, July 6-11, pp. 1-7, 2003